Transonic Airfoil Flow Simulation. Part II: Inviscid-Viscous Coupling Scheme

Alexandru DUMITRACHE*, Horia DUMITRESCU*, Florin FRUNZULICĂ*,**, Vladimir CARDOŞ*

*Corresponding author
*Institute of Mathematical Statistics and Applied Mathematics
Calea 13 Septembrie no. 13, 050711 Bucharest, Romania
alex_dumitrache@yahoo.com
**Department of Aerospace Engineering, University "POLITEHNICA" of Bucharest, 1 Gh.Polizu Street, Romania,
DOI: 10.13111/2066-8201.2010.2.3.3

Abstract: *A calculation method for the subsonic and transonic viscous flow over airfoil using the displacement surface concept is described. This modelling technique uses a finite volume method for the time-dependent Euler equations and laminar and turbulent boundary-layer integral methods. In additional special models for transition, laminar or turbulent separation bubbles and trailing edge treatment have been selected. However, the flow is limited to small parts of trailing edge-type separation. Comparisons with experimental data and other methods are shown.*

Key Words: transonic viscous flow, Euler equation, boundary layer.

1. INTRODUCTION

The current development of design algorithm for transonic airfoils follows two approaches. One approach is based on the solution of Navier-Stokes equation with structured and unstructured grids [1-4]. The second approach is one based on the interactive boundary layer theory and will form the basis for this work. This approach involves interaction between inviscid and boundary layer equations. For transonic flows, the inviscid flows is computed by a nonlinear potential method or by an Euler method and the viscous flow is computed by a boundary layer integral method [5-9]. This approach, though not as general as the Navier-Stokes approach, provides a good compromise between the efficiency and accuracy required in a design process.

The present approach consists of the iterative application of an unsteady finite-volume Euler method and a boundary layer part with semi-empirical models for separated regions using the displacement thickness concept. The inviscid flow method is discussed first, followed a description of the integral boundary-layer methods. The methods used to couple the viscid-invicid solutions is described, followed by computed results for supercritical flows over some airfoils for which experimental surface pressure and boundary-layer data are available.

2. BOUNDARY-LAYER METHOD

Viscous flow is simulated by coupling the inviscid code to a set of boundary-layer methods. The different boundary-layer methods as well as the iteration scheme are based on the reference [15]. In the present paper we will only sketch the basic ideas.

Laminar boundary-layer method. A two-dimensional compressible laminar boundary-layer integral method is used. This integral method uses for the evaluation of the integral thickness one parameter velocity profiles based on the Falkner-Skan solution of the boundary-layer equations. Compressibility effects are taking into account by means of the Stewartson-Illingworth transformation.

From the momentum equation and the moment of momentum equation with (ξ,η) thin shear layer coordinates we finally get the following system of equations:

$$\frac{d\theta}{d\xi}+\left(2+H-M_e^2\right)\frac{\theta}{U_e}\frac{dU_e}{d\xi}=\frac{C_f}{2} \tag{1}$$

$$\theta\frac{dH_{32}}{d\xi}+\left[2H^*+H_{32}\left(1-H\right)\right]\frac{\theta}{U_e}\frac{dU_e}{d\xi}=2C_D-H_{32}\frac{C_f}{2} \tag{2}$$

where

$$\delta_1=\int_0^{\eta_e}\left[1-\left(\rho U\middle/\rho_e U_e\right)\right]d\eta$$

$$\theta=\int_0^{\eta_e}\left(\rho U\middle/\rho_e U_e\right)\left[1-\left(U\middle/U_e\right)\right]d\eta$$

$$\delta_3=\int_0^{\eta_e}\left(\rho U\middle/\rho_e U_e\right)\left[1-\left(U^2\middle/U_e^2\right)\right]d\eta$$

$$\delta^*=\delta_1-\delta_{1,i}=\int_0^{\eta_e}\left(U\middle/U_e\right)\left[1-\left(\rho\middle/\rho_e\right)\right]d\eta$$

$$H=\delta_1\middle/\theta\ ,\ H_{32}=\delta_3\middle/\theta\ ,\ H^*=\delta^*\middle/\theta$$

with U_e - velocity at edge of boundary layer, δ_1 - displacement thickness, θ - momentum thickness, δ_3 - energy thickness, δ^* - density thickness and H - shape parameter, H_{32} - shape parameter for energy distribution, $C_{f,i}$ -incompressible skin friction coefficient, C_D - drag coefficient

To close the integral boundary-layer equations (1) and (2), the following functional dependencies are assumed:

$$H_{32}=\begin{cases}1.515+0.076\dfrac{\left(4-H_i\right)^2}{H_i}, & H_i<4\\[2ex] 1.515+0.040\dfrac{\left(H_i-4\right)^2}{H_i}, & H_i>4\end{cases} \tag{3}$$

$$\mathrm{Re}_\theta\frac{C_f}{2}=\begin{cases}-0.067+0.01977\dfrac{\left(7.4-H_i\right)^2}{H_i-1}, & H_i<7.4\\[2ex] -0.067+0.022\left(1-\dfrac{1.4}{H_i-6}\right), & H_i>7.4\end{cases} \tag{4}$$

$$\mathrm{Re}_\theta \frac{2C_D}{H_{32}} = \begin{cases} 0.207 + 0.00205\left(4 - H_i\right)^{5.5}, H_i < 4 \\ 0.207 - 0.003\dfrac{\left(H_i - 4\right)^2}{\left[1 + 0.02\left(H_i - 4\right)^2\right]}, H_i > 4 \end{cases} \tag{5}$$

$$H^* = \frac{\gamma - 1}{2} M_e^2 H_{32}, H_i = \frac{H - \dfrac{\gamma - 1}{2} M_e^2}{1 + \dfrac{\gamma - 1}{2} M_e^2} \tag{6}$$

Here H_i is the incompressible shape parameter of the velocity profile, Re_θ-Reynolds number based on momentum thickness

Transition, laminar separation and re-attachment criteria. The transition from laminar to turbulent boundary layer is a very complex phenomenon depending on several parameters. However, in the present method we only take care of pressure gradient, local Mach number and Reynolds number. Michel's empirical correlation modified by Smith-Gamberoni and Cebeci-Smith [11] is used:

$$\mathrm{Re}_{\theta,ts} = 1.174\,\mathrm{Re}_{\xi,ts}^{0.46},\ 2\cdot 10^5 < \mathrm{Re}_{\xi,ts} < 2\cdot 10^7 \tag{7}$$

Alternatively, transition can be specified by imput. Laminar operation is assumed if $C_f = 0$ during the laminar boundary-layer computation. The Goradia-Lyman's [12] criterion is then used to determine if either laminar stall or short bubble type separation is apparent:

$$-0.002\,\mathrm{Re}_\theta - 1 < \frac{dM_e}{d\left(\xi / c\right)} \tag{8}$$

where M_e - Mach number at the edge of boundary layer.

For short and long bubbles Horton's [13] correlations is used for the separation bubble length l_{sp}:

$$l_{sp} = \frac{5\cdot 10^4\ \theta_s}{\mathrm{Re}_{\theta,s}} \tag{9}$$

Inside the bubble $U_e^3\theta$ is assumed to be constant, leading to the reattachment momentum thickness:

$$\theta_R = \theta_s \frac{U_{e,s}^3}{U_{e,R}^3} \tag{10}$$

The model is available if bubble burst is indicated. After reattachment, the computation starts with the calculation of the turbulent boundary layer setting the shape parameter H to a value of 1.55.

Turbulent boundary layer. The turbulent boundary-layer method used for attached flow is essentially the lag-entrainment integral method of Horton [14], with suitable modifications for compressibility. It consists of the simultaneous integration of the momentum integral and entrainment equations together with a third empirical differential equation, which takes into account the effect upon the entrainment rate of the upstream history of the turbulence:

$$\frac{d}{d\xi}\left(\rho_e U_e^2 \theta\right) = \rho_e U_e^2 \left(\frac{C_f}{2} - \frac{\delta_1}{U_e}\frac{dU_e}{d\xi}\right) \tag{11}$$

$$\frac{d}{d\xi}\left[\rho_e U_e \left(\delta - \delta_1\right)\right] = \rho_e U_e C_E \tag{12}$$

$$\frac{dC_E}{d\xi} = \frac{0.014}{\theta}\left(C_{E,eq} - C_E\right) \tag{13}$$

The empirical shape parameter and entrainment relations used are based on those of Horton [15]:

$$H_i = \begin{cases} 0.88 + \left(\dfrac{0.591}{H_1 - 3.607}\right)^{0.4}, H_1 \geq 1.68 \\ 0.88 + \left(\dfrac{0.92326}{H_1 - 3.244}\right)^{1/1.85}, H_1 < 1.68 \end{cases} \tag{14}$$

where $H_1 = \left(\delta - \delta_1\right)/\theta$ is Head's shape parameter and

$$H_1 = \frac{0.057}{H_1 - 3.0}\frac{C_f}{C_{f,i}} \tag{15}$$

In order to prevent the failure of the calculation due to the inability of standard boundary-layer methods to compute boundary-layer parameters beyond separation, a constant value of the entrainment coefficient $C_{E,eq}$ that corresponds to a shape parameter $H_{i,s} = 4$ is used.

The length scale θ in Eq. (13) is set equal to the value of θ at separation shear layer. The momentum equation is removed and θ and δ_1 are calculated from the computed values of $\left(\delta - \delta_1\right)$. Skin function C_f is calculated from a compressible form of the Ludwieg-Tillman relation:

$$C_f = \left(\frac{C_f}{C_{f,i}}\right) C_{f,i} = \frac{0.246}{\left(1 + 0.13M_e^2\right)\mathrm{Re}_\theta^{0.268}\, 10^{-0.678 H_2}} \tag{16}$$

where

$$\mathrm{Re}_\theta = \frac{\rho_e U_e \theta}{\mu_e}, \frac{C_f}{C_{f,i}} = \left(1 + 0.130M_e^2\right)^{-1} \tag{17}$$

The casual reattachment is simulated by evaluating $dH_i/d\xi$ at each step in the separated flow from the shape parameter equation (Eq.(6)), and allowing H_i to become less than $H_{i,s}$ once the derivative becomes negative. But, in general, the application of the above numerical method is limited to flows where the turbulent boundary layer is attached over the airfoil surface except for small portions.

2.1 INVISCID-VISCOUS COUPLING SCHEME

A cyclic iterative procedure between the inviscid flow method and the boundary-layer part is used to finally provide the convergent viscous solution.

Both regions are computed separately but sequentially until both are converged to solution with common boundary values. The following sequence is used:

1) firstly, the inviscid solution is computed for the equivalent airfoil shape (initially, a flat plate δ_1 distribution is used);

2) then, after ten Euler cycles (until the left coefficient do not vary significantly), the displacement thickness distribution is computed for the given pressure distribution by means of the viscous method previously described;

3) the under-relaxed displacement thickness

$$\delta_1 = \delta_{1,old} + \omega\left(\delta_{1,new} - \delta_{1,old}\right) \tag{18}$$

is added to the physical shape and for this shape the inviscid flow field is computed again, using ten Euler cycles;

4) then, new viscous quantities are computed and the whole cycle between viscous and inviscid computations is continued until either the convergence criterion is reached or the cycle is stopped by the user. The convergence criterion is based on the relative difference between the left coefficients in two consecutive cycles; the calculation is stopped when this difference reaches a bound.

In the present method some empirical feature has been introduced to deal with the trailing edge region. Thus, it has been assumed that C_f is equal zero just at the trailing edge and the pressure distribution of the aft part of the airfoil are forced to satisfy this condition.

2.2 FORCE AND MOMENT CALCULATION

Lift and moment coefficients are computed by integrating the surface pressure and skin friction.

Concerning the drag, there are in principle two possible ways of estimating the overall drag of the airfoil, which may be termed near field and far field approaches. In the former, one calculates separately the skin friction drag $\left(C_{D,F}\right)$ by the boundary-layer method and the pressure drag $\left(C_{D,P}\right)$ by integrating the stream wise component of the surface pressure, and then the total drag is given by adding the two components:

$$C_D = C_{D,F} + C_{D,P} \tag{19}$$

In the later, the drag is obtained from the momentum thickness of the wake downstream of the airfoil comuted using the approach of Squire and Yang [15] $\left(C_{D,V} = 2\theta_\infty / c\right)$ and adding the losses through the shock $\left(C_{D,W}\right)$, that is

$$C_D = C_{D,V} + C_{D,W} \tag{20}$$

For subcritical (or shock-free) flows it was found that both methods gave the same result, while in supercritical flows the integration of skin friction and pressure seems to underpredict the drag compared with the second approach (far field) and also with

measurements. In the present method, no computation through the wake is needed due to the special trailing edge treatment.

3. RESULTS AND DISCUSSION

Generally, the results presented here have been obtained using a computational "O" grid with 280x60 points. The solution was obtained with a residual of 10^{-6} in the inviscid part and a convergence criterion

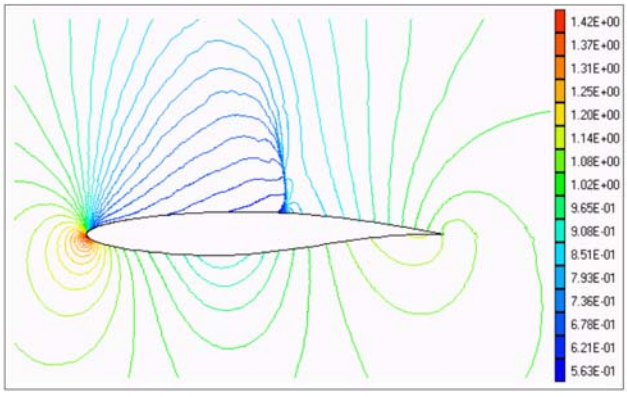

i)

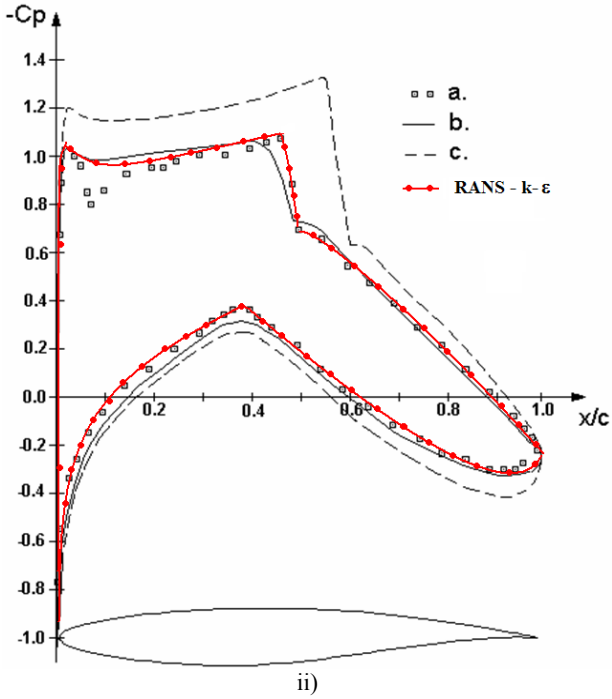

ii)

Fig. 1 – Pressure coeficient: i) isolines and ii) distribution for the RAE2822 airfoil: $M_\infty = 0.725$, $\mathrm{Re} = 6.5 \cdot 10^6$, $\alpha_{\exp} = 2.3^0$: (a) experiment, (b) inviscid – viscous method and (c) inviscid solution (Euler) of $\Delta C_L \cong 0.1\%$ for the interacting cycle.

We start with some calculations for the RAE 2822 airfoil. A number of cases have been extensively tested. We have chosen the case: $M_\infty = 0.725$, $\mathrm{Re} = 6.5 \cdot 10^6$, $\alpha_{\exp} = 2.3^0$, transition point at 3%.

Figure 1 shows a comparison of the pressure coefficient distribution calculated without and with boundary layer and experiment. The overall agreement between theory and experiment is relatively good.

Figure 2 shows the displacement thickness distribution (i) and the skin function distribution (ii). It can note that the rapid growth of the boundary layer due to the pressure rise through the shock.

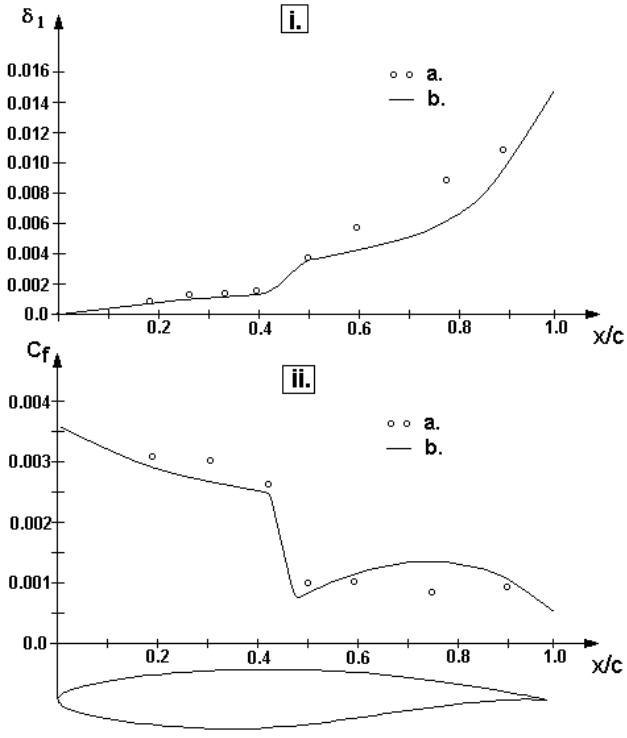

Fig. 2 – (i) Displacement thickness distribution for RAE2822 airfoil; (ii) skin friction distribution: (a) - experiment, (b)- inviscid-viscous method.

As a second example calculating are presented for the NACA 0012 airfoil. Flow condition are $M_\infty = 0.7$, $\mathrm{Re} = 9 \cdot 10^6$ and transition at 5%. Calculations have been performed at several values of C_L corresponding with test cases [15]. Figure 3 gives the $C_L - \alpha$ and $C_L - C_D$, curves obtained in comparison with the experimental results. However, in the neighborhood of $\alpha = 4^0$ the calculations show numerical problems due to the amount of flow separation probably becomes too large. A good agreement is found.

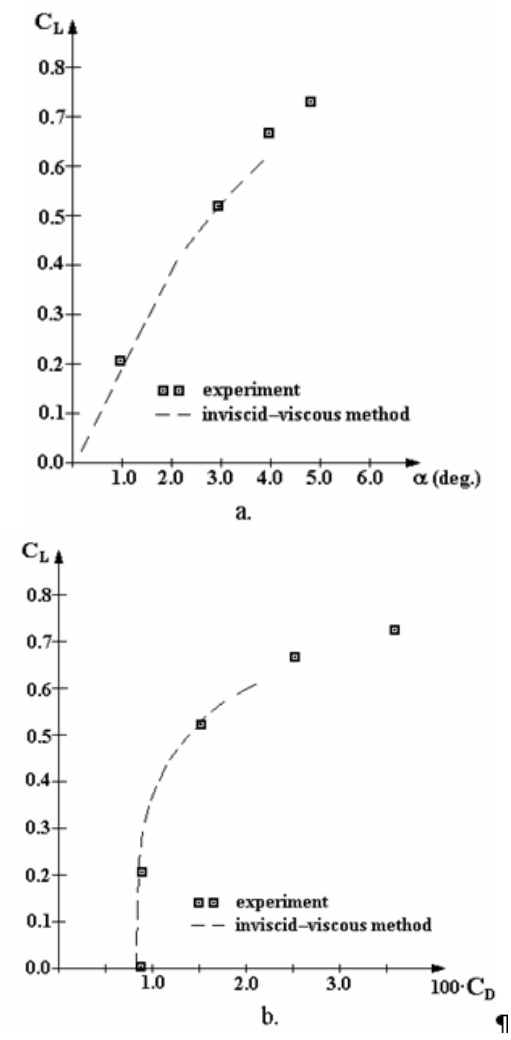

Fig. 3 – $C_L - \alpha$ (a) and $C_L - C_D$ (b) curves compared with experiment for NACA0012 airfoil

4. CONCLUSIONS

An interactive method was presented for the viscous transonic flow analysis. It seems to be a good engineering tool for the analysis of airfoil in transonic flow due to its accuracy and fast resolution using a simple self-consistent formulation. Compared with other methods it seems to have the following advantages:

1. a sequentially Euler/integral boundary layer coupling technique;
2. a viscous model which includes the laminar boundary layer part and transition as well as separation models;
3. a fairly simple formulation to deal with the trailing edge which accounts in an accurate way for the effects of the wake.

REFERENCES

[1] T.L. Holst, U. Kaynak, K.L. Grundy, Transonic wing flows using an Euler/Navier-Stokes zonal approach., *Journal of Aircraft*, vol.**24**, no.1, pp 17-24.,1987

[2] A. Jameson, N.A. Pierce and L. Martinelli, *Optimum aerodynamic design using the Navier-Stokes equations*, AIAA Paper 97-0101, 1997.

[3] M. Jayaram and A. Jameson, *Multigrid solution of Navier-Stokes equations for flow over wings*, AIAA Paper 88-0705, 1988.

[4] D. Mavriplis and A. Jameson, Multigrid solution of the Navier-Stokes equations on triangular meshes, *AIAA Journal*, vol.**28**, pp. 1415-1425, 1990.

[5] R.C. Lock and B.R. Williams, Viscous-inviscid interactions in external aerodynamics, *Progress Aerospace Sciences*, 24, pp. 51-171, 1987.

[6] R.E. Melnik, R.R Chow, H.R. Mead and A. Jameson, *An inproved viscid/inviscid interaction procedure for transonic flow over airfoils*.- NASA CR-3805, 1985.

[7] W. Schmidt, A. Jameson and D.D. Whitfield, *Finite volume solutions for the Euler equations for transonic flow over airfoils and wings including viscous effects*, AIAA Paper 81-1265, 1981.

[8] M. Drela and B.B. Giles, Viscous-inviscid analysis of transonic and low Reynolds number airfoils, *AIAA Journal*, vol.**25**, pp.1347-1355, 1987.

[9] D.P. Coiro, M. Amato and P. De Matteis, Numerical predictions of transonic viscous flows around airfoils through an Euler/boundary layer interaction method, *Aeronautical Journal*, pp.157-165, 1992.

[10] S. Leicher, *Viscous flow simulation on high lift devices at subsonic and transonic speed*, AGARD Conf Proc 291, pp. 6.1-6.15, 1980.

[11] T. Cebeci, *An engineering approach to the calculation of aerodynamic flows*, Springer-Verlag, 1999.

[12] S.H. Goradia, V. Lyman, Laminar stall prediction and estimation of $C_{L,\max}$, *Journal of Aircraft*, vol. **11**, pp. 528-536, 1974.

[13] H.P. Horton, *Laminar separation bubbles in two and three dimensional incompressible flow*, PhD Thesis, Queen Mary College, University of London, 1967.

[14] H.P. Horton, *Entrainment in equilibrium and non-equilibrium turbulent boundary layers,* Hawker Siddeley Aviation Ltd, Hartfield, Rep Research/1094/HPH, 1969.

[15] P.H. Cook, M.A. McDonald and M.C.F. Formin, *Airfoil RAE 2822 pressure distribution and boundary layer measurements,* AGARD-AR-138, 1979.